Revision notes

We are grateful to the valuable comments and suggestions from the referee 2 on our manuscript. The paper has now been corrected and improved. The detailed responses to their questions are listed bellows.

1. Specific comments Line 313 and Table 1: X2Cd represents out-sphere complexes. The complex stability constant (logKX2Cd) for out-sphere complexes should be small and much lower than these for inner-sphere complexes. However, the data is great (8.3) and greater than these for inner-sphere complexes in Table 1. I cannot understand this data. Please provide more explanations.

Response: The calculated logK for (X2Cd) and (SOCd) in this study are comparable to the data reported in earlier literatures. For example, Barbier et al. (2000) showed the logK(X2Cd) and logK(SOCd) values of 5.61 and 2.44, respectively. For other metallic ions such as Zn^{2+} and Pb^{2+} (Bradbury and Baeyens, 1991), Ni^{2+} (Marcussen et al., 2009), Cu^{2+} (Stader and Schindler, 1993), logK(X2Me)> logK(SOMe) was also observed.

To the best of our knowledge, only XAS observations can determine the binding environments of metallic ions whether are inner-sphere/or outer sphere, e.g., monodentate complexation, or bidentate edge-sharing or corner-sharing complexes, to SOH/other sites. The SCM model finds that some specific Cd complexes give the best model fit, but it is well known that the actual molecular-level complexation determined by XAS rarely matches the 'best' SCM model fit (because the SCM simply gives the simplest fit solution). In other word, X2Cd+ in the model fits can't be recognized as simple outer-sphere complexes, neither the SOH can be considered as the inner-sphere

complexes. Thus, it is better to avoid using "inner-sphere" and "outer-sphere" to describe the SOCd and X2Cd+ species just based on SCM. Throughout the revised paper, we have clarified it.

2. Lines 409-424 (Discussion section): Authors cited the results of the composites of iron (hydr)oxides with bacteria in literature for comparison. While, in Introduction section, authors also mentioned that the model was used for Cd adsorption onto composite of kaolinite with bacteria. Therefore, in addition to the results of the composites of iron (hydr)oxides with bacteria, authors were suggested to compare their results with these of composite of kaolinite with bacteria. Because the surface chemical properties of montmorillonite were opposite to these of (hydr)oxides, but similar to kaolinite.

Response: The "discussion" will be more complete if a comparison between 1:1 and 2:1 clay-bacteria composites is involved. This part has been given in the revised version.

3. In the section of Environmental Implication: please provide some examples of Cd contaminated soils with montmorillonite as major clay mineral in temperate regions to show practical significance of this study.

Response: It has been given in the revision

4. Line 407: do not repeat the data in the section of Results (69.1%:30.9%)

Response: It has been deleted, and this sentence has been re-written.

5. Figure S2: Please provide the AFM images of single montmorillonite, single bacteria and their composite for reader to find the attachment of bacteria on montmorillonite. At present, it is difficult to distinguish bacteria from the composite from the images.

Response: We have provided the single montmorillonite and bacteria images, by the way we also chose new images for the binary montmorillonite-*B .subtilis* composites, and now it is easier to distinguish each component.

6. Line 245: "binding constant" should be "binding stability constant".

Response: It has been revised.

7. Lines 313 and 336: "Complexation constant" should be "complex stability constant".

Response: It has been revised.

8. English corrections Line 192: change "finial" to "final".

Response: It has been revised.

9. Line 215: some words need to be added after "of".

Response: It has been revised.

10. Line 246: "was" should be "were".

Response: It has been revised.

11. Line 247: change "mol/g" to "mol g-1".

Response: It has been revised.

12. Line 317: "sdsorption" should be "adsorption".

Response: It has been revised.

Surface complexation modeling of Cd(II) sorption to montmorillonite, bacteria, and their composite

Ning Wang[1,2]*, Huihui Du[1,2]*, Qiaoyun Huang[1,2]**, Peng Cai [1,2], Xingmin Rong[2] and Wenli Chen[1,**]

[1] State Key Laboratory of Agricultural Microbiology, Huazhong Agricultural University, Wuhan 430070, China.

[2] Key Laboratory of Arable Land Conservation (Middle and Lower Reaches of Yangtze River), Ministry of Agriculture, College of Resources and Environment, Huazhong Agricultural University, Wuhan 430070, China.

*These authors contributed equally to this work.

**Corresponding author: Q. Huang, E-mail: qyhuang@mail.hzau.edu.cn; W. Chen, wlchen@mail.hzau.edu.cn; Tel: +86-27-87671033; Fax: +86-27-87280670

Abstract

Surface complexation modeling (SCM) has emerged as a powerful tool for simulating heavy metal adsorption processes on the surface of soil solid components under different geochemical conditions. The component additivity (CA) approach is one of the strategies that have been widely used in multi-component systems. In this study, potentiometric titration, isothermal adsorption, zeta potential measurement, and extended X-ray absorption fine structure (EXAFS) spectra analysis were conducted to investigate Cd adsorption on 2:1 clay mineral montmorillonite, on Gram-positive bacteria *Bacillus subtilis*, and their mineral-organic composite. We developed constant capacitance models (CCM) of Cd adsorption on montmorillonite, bacterial cells, and mineral-organic composite. The adsorption behavior of Cd on the surface of the composite was well explained by CA-SCM. Some deviations were observed from the model simulations at pH < 5, where the values predicted by the model were lower than the experimental results. The Cd complexes of X_2Cd, $SOCd^+$, $R\text{-}COOCd^+$, and $R\text{-}POCd^+$ were the predominant species on the composite surface over the pH range of 3 to 8. The distribution ratio of the adsorbed Cd between montmorillonite and bacterial fractions in the composite as predicted by CA-SCM closely coincided with the estimated value of EXAFS at pH 6. The model could be useful for the prediction of heavy metals distribution at the interface of multicomponents and their risk evaluation in soils and associated environments.

Keywords: montmorillonite, bacteria, composite, Cd(II), sorption, modeling

1. Introduction

Anthropogenic activity and industrialization release large quantities of heavy metals into soils (Fomina and Gadd, 2014; He and Chen, 2014). The interactions between soil solid components and heavy metals in complex natural systems should be understood in order to predict their transport and fate. Surface complexation modeling (SCM) is a powerful tool for describing adsorption processes and mechanisms under different geochemical conditions (Dong and Wan, 2014; Wang and Giammar, 2013). SCM has been adopted to simulate the adsorption of heavy metals on the surface of soil solid components such as kaolinite (Angove et al., 1997), montmorillonite (Akafia et al., 2011; Benedicto et al., 2014; Bradbury et al., 2005; Ikhsan et al., 2005; Soltermann et al., 2014), magnetite (Kim et al., 2012), manganese oxide (Wang et al., 2013), fulvic and humic acid (Christl et al., 2001; Koopal et al., 2005; Milne et al., 2003), natural organic matter (Koopal et al., 2005; Gustafsson et al., 2014), and bacteria (Borrok and Fein, 2005; Borrok et al., 2004; Daughney et al., 2001; Fein et al., 2001; Kenney and Fein, 2011; Liu et al., 2013; Moon and Peacock, 2011).

Soil solid components, which include bacteria and clay minerals, often exist as composites in natural environments. The component additivity (CA) approach has been widely used in the application of surface complexation models for describing heavy metal adsorption on mixtures and on the composites of soil solid components. The component additivity-diffuse layer model (CA-DLM) has been successfully applied to model the adsorption of Co^{2+} (Landry et al., 2009), Cd^{2+} (Reich et al., 2010), and Pb^{2+} (Reich et al., 2010), on mixtures of hydrous ferric oxide (HFO) and quartz with kaolinite. Dong and Wan (2014) indicated that the CA-SCM can provide excellent

predictions for uranium (VI) adsorption on quartz-sand dominated sediments. Fowle and Fein (1999) concluded that the CA approach can be used to model the adsorption of Ca^{2+}, Cu^{2+}, Cd^{2+}, and Pb^{2+} on mixtures of *Bacillus licheniformis* and *B. subtilis*. Additionally, CA could successfully describe Cd, Co, Sr, and Zn adsorption onto the mixtures of 10 species of Gram-positive bacteria (Yee and Fein, 2001). For the mixtures of minerals and organic systems, the extended constant capacitance model was used to depict Cd^{2+} adsorption onto goethite, kaolinite, and muloorina illite in the presence of citric acid (Lackovic et al., 2004a,b). The linear additivity model has succeeded in predicting Cu^{2+} adsorption, but has failed to simulate Ca^{2+} adsorption on goethite in the presence of fulvic acid (Weng et al., 2008). The adsorption of Cd^{2+} onto *Comamonas spp.*–ferrihydrite composite could be accurately predicted by the addition of the reaction between end-member ferrihydrite and bacteria (Song et al., 2009). However, the amount of Cd^{2+} adsorption onto the composite was up to 10% lower than that predicted by the additive approach. In the study of Alessi and Fein (2010) the CA approach was applied to describe the extent of Cd adsorption on the surface of two- and three-component mixtures of *B. subtilis* cells, HFO, and kaolinite at various mass ratios in the presence of acetate. The models matched well with experimental data in the absence of acetate, whereas they underestimated Cd adsorption in the presence of acetate. Moon and Peacock (2013) found that Cu adsorption behavior on ferrihydrite–*B. subtilis* composites with ferrihydrite as the major component can be modeled by a component additivity approach. By contrast, composites with a majority of bacteria component cannot be simulated by a component additivity approach, and significant

deviations were observed.

Previous studies concerning surface complexation models have mainly focused on heavy metal adsorption by individual minerals or bacteria or mineral–organics and metal oxide–bacteria composites. To the authors' knowledge, no SCM investigation using 2:1 clay mineral–bacteria composites, has been performed. Montmorillonite, a representative of the 2:1 phyllosilicates, exhibits large specific surface area and high cation exchange capacity, which make it an effective adsorbent for heavy metals. The clay mineral is widely distributed in a variety of soils in temperate zone. The model developed in clay mineral–bacteria composites will provide insights into the behaviors of heavy metals in contaminated soils of these regions. Thus, in this study, we first develop surface complexation models for Cd adsorption on end-member 2:1 clay mineral montmorillonite, Gram-positive bacteria *Bacillus subtilis*, and finally their mineral-organic composite by using the component additivity (CA) approach. Moreover, linear combination fitting of the extended X-ray absorption fine structure (EXAFS) spectra were applied to verify the distribution ratio of Cd between different components derived from CA-SCM.

2. Materials and Methods

2.1. Adsorbent

Montmorillonite, (Sanding Group Co. Ltd., Shaoxing, Zhejiang, China), was prepared following previously outlined procedures (Hong et al., 2012; 2013). The clays were oxidized using H_2O_2 (30%) to remove any residual organic matters. The < 2 μm

colloidal fractions were isolated through sedimentation. The specific surface area, determined by the BET method (N_2 adsorption), was found to be 60.2 m^2 g^{-1}. Previous study showed that a particle was estimated to be formed of nearly 20 stacked layers in the dehydrated state used in the gas adsorption experiment (BET' method), whereas it was estimated to be composed of only 1 or 2 layers in aqueous suspension (Tournassat et al., 2003). Thus, the values derived from BET' method usually underestimate the actual total surface area in aqueous. Herein, we set the SSA of montmorillonite to be 800 m^2 g^{-1}, and the detailed processing procedures are shown in Supporting Information.

The test bacteria used in this study came from the aerobic Gram-positive species *B. subtilis*, which were obtained from the State Key Laboratory of Agricultural Microbiology. The microorganisms were inoculated into 10 mL LB medium and cultured for 7 h at 28 ℃ to reach the exponential phase with an optical density of 1.4 at 600 nm (OD600 nm). Subsequently, 2 mL of the resulting bacterial suspension was transferred to 200 mL LB medium for another 18 h inoculation (OD_{600nm}=2.7) to reach the mid-exponential phase. Cells were pelleted by centrifugation at approximately 7200 *g* for 5 min and rinsed three times in ultrapure water. The ratio of the wet weight to dry (60 ℃ in drying oven) weight of the biomass is 9:1. The biomass mentioned in this paper all refer to dry weight.

Montmorillonite and the bacterial cells were suspended in 0.01 M $NaNO_3$ to produce the suspensions that were used in the experiments. The montmorillonite– bacteria composite was prepared following a montmorillonite: *B. subtilis* mass ratio of 7:1 to produce suspensions (4 h, 28 ℃). The resultant montmorillonite–bacteria

composite suspensions were used for subsequent experiments. Preliminary isothermal adsorption (pH 8) of bacteria to montmorillonite results showed that the maximum adsorption predicted by Langmuir equation was approximately 0.14 g (dry cell)/ g (clay) which was equal to a mass ratio (clay to bacteria) of 7:1 (Supporting Information, Fig. S1). Clearly adsorption of bacteria on montmorillonite decreased with the increase of pH, thus bacteria can be completely adsorbed by montmorillonite to a large extent in all experimental conditions (pH 3–8.5) at this ratio. The bacterial cells were remain intact under the experimental condition (see AFM images of the Supporting Information, Fig. S2).

2.2. Reagents

Analytical reagent grade chemicals were used throughout the study. $Cd(NO_3)_2$ was used to prepare 178.0 μmol L^{-1} Cd(II) stock solution. Water was Milli-Q reagent grade.

2.3. Zeta potential analysis

Zeta potential analysis was conducted to study the surface charge properties of montmorillonite, *B. subtilis,* and montmorillonite–*B. subtilis* composite. Suspensions were prepared the same as section 2.1, over the pH range of 3 to 8. Samples were injected into a zeta potential analyzer (Zetaplus90, Brookhaven), and measured in triplicate.

2.4. Potentiometric titrations

Titration experiments were performed (in duplicate) according to the procedures described by Fein et al. (2005). The suspensions (1 g L^{-1}, 40 mL) of montmorillonite and *B. subtilis* and the composite in 0.01 M $NaNO_3$ were placed in a sealed titration vessel maintained under a positive pressure of N_2. Titrations were conducted using an automatic potentiometric titrator (Metrohm titrator 836, Switzerland). Each suspension

was first titrated to pH 3 by using 0.1136M HNO_3 solutions and then to pH 8.5 by using

0.0976 M NaOH. At each titration step, a stability of 0.01 mV S^{-1} was attained before

adding the next drop of the titrant.

Gran plot was adopted to determine the specific volume of titrant added at the

equivalence point (*Ve*) and to derive the total H^+ concentration (TOTH) (Chu et al.,

2002; Du et al., 1997; Liu et al., 1999; Liu et al., 2013).

The values for the Gran function (G) were calculated as follows:

On the acidic side: $G_a = (V_0 + V_{at} + V_b) \times 10^{-pH} \times 100$

On the alkaline side: $G_b = (V_0 + V_{at} + V_b) \times 10^{-(13.8-pH)} \times 100$

Gran plots for titration data on montmorillonite and *B. subtilis* are illustrated in

Fig. S3, where V_0 stands for the initial volume of the titrimetric suspension; and V_a and

V_b represent the total volume of acid and alkaline solution added at each titration point,

respectively. In the Gran plots, the OH^- added to a suspension firstly neutralizes the

excess H^+ before V_{eb1}, then reacts with the functional group on the surface of the sorbent

between V_{eb1} and V_{eb2}, finally changes the pH after V_{eb2}. No apparent surface reactions

consuming OH^- before V_{eb1} were noted. The total concentration of reacting H^+ at each

titration point (TOTH) was calculated using the following equation, where C_b stands

for NaOH concentration:

$$TOTH = \frac{-(V_b - V_{eb1}) \times C_b}{V_0 + V_{at} + V_b} \ (mol \ L^{-1}),$$

2.5. Adsorption experiment

The adsorption edge experiments were conducted in 0.01 M $NaNO_3$ solutions to

investigate the adsorption of Cd onto montmorillonite, *B. subtilis* and the composite.

15 mL 178.0 μmol L^{-1} Cd(II) solution and 15 mL 2 g L^{-1} adsorbent suspensions were added to 50 mL centrifuge tubes. A suitable volume of concentrated HNO$_3$ or NaOH solutions was added to adjust the pH of the suspensions from 3 to 8. The final concentration of Cd and adsorbents were 89.0 μmol L^{-1} and 1 g L^{-1}, respectively. Fixed pH isotherm experiments were performed at pH 6 and 8 in 0.01 M NaNO$_3$ electrolyte. The initial concentrations of Cd ranged from 8.9–89.0 μmol L^{-1} with a sorbent concentration of 1 g L^{-1}. The mixtures were allowed to equilibrate for two hours at 28 ℃. After equilibration, the final suspensions were centrifuged at 12557 g for 5 min, and the clear supernate was analyzed using atomic adsorption spectroscopy (AAS; Varin AAS240FS) to determine the residue Cd.

Solution speciation of 89.0 μmol L^{-1} Cd(II) in 0.01M NaNO$_3$ was calculated as a function of pH using the geochemical software Visual MINTEQ 3.1. Cd^{2+} was determined to be the main species at the experimental conditions. Cd(OH)$_2$, CdOH$^+$, and Cd$_2$OH^{3+} were also found at pH > 7.8, but in relatively small percentages.

2.6. X-ray absorption spectroscopy

We selected pH 6 sample of the adsorption edge experiments in section 2.5 as representative to perform the XAS experiments. The solid phases after centrifugation were transformed immediately to collect XAS spectra in 12 h. The sample holders were packed together with moist tissues (stored at ~ -4° C) to minimize sample drying during shipment to the Shanghai Synchrotron Radiation Facility (SSRF), China. The X-ray absorption data at the Cd K-edge (~26700 keV) of the samples were recorded at room temperature in the fluorescent mode with silicon drift fluorescence detector. The station was operated with a Si(III) double crystal monochromator. During the measurement,

the synchrotron was operated at energy of 3.5 GeV and a current between 150–210 mA. EXAFS spectra were collected from 26511 to 27551 eV. Background subtraction and normalization of the XAS data were conducted in ATHENA, a program in the IFEFFIT package (Ravel and Newville, 2005). The background subtraction was performed using PySpline. The pre-edge was fit to a linear function and the post-edge background to two 2nd-order polynomial segments. To obtain information on the partitioning of Cd between the different fractions of the composites, the spectra were fitted using a linear combination fitting procedure (LCF). Cd-adsorbed montmorillonite, Cd-bacteria were used as end-member for the 2-component fitting of the binary composites, with linear combination performed over the k^3-range of 2.3-10 Å^{-1} (force weight to sum to 1). The goodness of the fitting was evaluated by the best-fit criterion values (R) (Du et al., 2016).

2.7. Surface complexation modeling

The program FITEQL 4.0 was utilized to determine functional group site concentrations, proton, and metal binding stability constants (Herbelin and Westall, 1999). A constant capacitance model was implemented (Tertre et al., 2006). The activity coefficient correction was made within FITEQL using the Davies equation. An indicator of the goodness of the fitting is the overall variance, V, in Y (Herbelin and Westall, 1999). $V_Y = \dfrac{WSOS}{DF}$, where WSOS is the weighted sum of squares of the residuals and DF is the degrees of freedom. Lower V_Y values signify better fits. The systematic process of developing the SCM was started by fitting the model to the experimental data for montmorillonite and *B. subtilis*.

The potentiometric titration data was fit to generate the acid-base constants and surface site densities (Fig. S4). Acid-base reactions on the surface of montmorillonite

are represented by the following equations:

$$SOH \Leftrightarrow SO^- + H^+ \tag{1}$$

$$SOH + H^+ \Leftrightarrow SOH_2^+ \tag{2}$$

$$WOH \Leftrightarrow WO^- + H^+ \tag{3}$$

$$X^- + H^+ \Leftrightarrow XH \tag{4}$$

$$X^- + Na^+ \Leftrightarrow XNa \tag{5}$$

where SOH and WOH are aluminol and silanol sites on the surface of montmorillonite, respectively. X^- is the negative exchange site that can react with both H^+ and Na^+. The total concentration of exchange site and the binding stability constants of XH, XNa were used as fixed input parameters when the titration data were fitted. These three values were 8.7×10^{-4} mol g^{-1}, -2.2 and 1.4, respectively (Table S1), which come from Tertre et al. (2006) and Soltermann et al. (2014). The acid-base constant and the site density of SOH and WOH were set as iterated parameters, in addition, these parameters were iterated simultaneously.

The acid-base reactions on the surface of *B. subtilis* were represented by

$$R\text{-}L_iH^0 \Leftrightarrow R\text{-}L_i^- + H^+ \tag{6}$$

where R represents the bacterium to which each functional group is attached. Carboxyl sites, phosphate sites, and hydroxyl sites were considered to be the main functional groups on the surface of *B. subtilis* (Yee and Fein, 2001). L_iH^0 represents these three groups.

Acid-base equilibrium constants and site densities (Tables S1 and S2) were used as fixed input parameters in the modeling of the Cd pH adsorption edge and fixed pH

isotherm data. The constants of Cd complexes with the functional groups on each sorbent were iterated simultaneously. The following equilibria were used to describe Cd(II) adsorption onto montmorillonite:

$$2X^- + Cd^{2+} \Leftrightarrow X_2Cd \tag{7}$$

$$SOH + Cd^{2+} \Leftrightarrow SOCd^+ + H^+ \tag{8}$$

Due to their higher pK_a, hydroxyl sites are not deprotonated over the range of pH 3 to 8. To simplify the model, hydroxyl sites were not invoked. Cd(II) adsorption on *B. subtilis* was described with the following reaction equilibria:

$$R\text{-}COO^- + Cd^{2+} \Leftrightarrow R\text{-}COOCd^+ \tag{9}$$

$$R\text{-}PO^- + Cd^{2+} \Leftrightarrow R\text{-}POCd^+ \tag{10}$$

Finally, we combined the model of Cd(II) adsorption on montmorillonite and *B. subtilis* to simulate the adsorption behavior of Cd(II) on the composite. End-number montmorillonite and *B. subtilis* models were combined in FITEQL 4.0 using the CA approach.

3. Results

3.1. Zeta potential

The zeta potential of montmorillonite, *B. subtilis,* and montmorillonite–*B. subtilis* composite are given in Fig. 1. Over the whole pH range studied, both montmorillonite and the composite had negative surface charge with very low pH_{pzc} around pH 3.1. The bacteria displayed a negative surface charge at pH > 3.5 and had a higher pH_{pzc} than the

value reported by Fein et al. (2005) ($pH_{pzc} < 2$). The negative electrokinetic charge of all sorbents increased with pH and remained constant when pH was higher than 5. The zeta potential of montmorillonite and bacteria were -2.29 mV and 12.27 mV at pH 3, -26.70 mV and -19.46 mV at pH 8. The surface of the montmorillonite–bacteria composite was more negatively charged than that of montmorillonite and *B. subtilis* at pH > 5, the zeta potential of the composite was -20.30 mV at pH 3.

3.2. Cadmium adsorption

Figure 2 shows the pH dependence of Cd adsorption on montmorillonite, *B. subtilis*, and montmorillonite–*B. subtilis* composite. Adsorption onto montmorillonite increased slowly over the pH ranges, and about 55% of the total Cd(II) was adsorbed at pH 8. Adsorption onto *B. subtilis* increased sharply between pH 3 and 7 and then reached a plateau at pH 7–8. Nearly 90% of total Cd(II) was adsorbed at pH 8. In comparison to bacteria, the uptake of Cd on montmorillonite–*B. subtilis* composite increased more slightly over the range of pH 3 to 8. The extent of adsorption onto the composite increased swiftly from pH 3 to 5, and varied slightly at pH 5–8. About 60% of the total Cd(II) ions were adsorbed onto the composite at pH 8.

3.3. Modeling of Cd adsorption onto montmorillonite and *B. subtilis*

The titration data for montmorillonite and *B. subtilis* are presented in Fig. S4. Bacteria exhibited significant buffering capacity over the range of pH 3 to 8.5, which was assigned to the deprotonation of functional groups on cell walls (Borrok et al., 2004; Moon and Peacock, 2011; Yee and Fein, 2001). Montmorillonite presented strong buffering capacity only at pH < 4 and pH > 7.5. This result was in line with the report of Ikhsan et al. (2005), which also showed similar buffering behaviors of a Ca-

montmorillonite over these pH ranges. The titration data of montmorillonite and *B. subtilis* were successfully modeled with reactions (1)–(5) and (6). The protonation constants and site densities of sorbents calculated from titration data are indicated in Tables S1 and S2.

Adsorption of Cd onto the surface of montmorillonite and *B. subtilis* were successfully modeled with reactions (7)–(10). The best-fit for cadmium adsorption on montmorillonite is depicted in Fig. S5 (a). The adsorption of Cd(II) onto montmorillonite was modeled using two adsorbed species, X_2Cd and $SOCd^+$. The calculated complex stability constants of these two species were 8.30 and -1.68, respectively (Table S1). The complexation of Cd(II) onto two X^- sites (X_2Cd) dominated at pH < 4.5 while monodentate complexation onto SOH sites of the crystal edges ($SOCd^+$) predominated at pH > 4.5. The V_Y value of the model which describes the Cd adsorption on montmorillonite was 5.6. The best-fit model for the Cd adsorption onto *B. subtilis* is presented in Fig. S5 (b). The optimized $logK_{R-COOCd+}$ and $logK_{RPOCd+}$ values were 2.54 and 2.87, respectively (Table S2). Surface complexation model successfully simulated the adsorption edge of *B. subtilis* over the pH ranges of 3 to 8. The model predicted that one inner-sphere monodentate complexation ($R-COOCd^+$) dominated at low pH while another inner-sphere monodentate complexation ($R-POCd^+$) dominated at high pH. The V_Y value of the model which described the Cd adsorption on bacteria was 3.8.

3.4. Modeling of Cd adsorption onto montmorillonite–*B. subtilis* composite

The parameters for the model of Cd adsorption onto montmorillonite–*B. subtilis* composite are shown in Table 1. As per the CA approach, the constants for protonation

and the acid-base reactions on the surface of the composite were the same as those for the end-member montmorillonite and *B. subtilis*. The operational site densities of functional groups used in the model of Cd sorption on the composite were calculated based on the end-member site densities weighted to the montmorillonite:bacteria mass ratio (Moon and Peacock, 2013). The specific capacitance and surface area were calculated in the same way. Four Cd complexation species were considered in the model of Cd sorption on the composite, i.e., X_2Cd and $SOCd^+$ on montmorillonite; two inner-sphere complexes on bacteria. The complexation constants of the four species were the same as those optimized by the models of Cd adsorption on montmorillonite and *B. subtilis*.

The adsorption behavior of Cd on montmorillonite–*B. subtilis* composite was well described by CA-SCM, except some deviations were observed at pH < 5 (Fig. 3, V_Y=15.4). The complex X_2Cd dominated below pH 4. At pH 4.5, the $SOCd^+$ was the major species with deprotonation of the SOH surface sites. At pH 3–5.5, the inner-sphere complex $R-COOCd^+$ on the surface of bacteria contributed 10–20% of the total Cd adsorption. At pH above 5.5, the inner-sphere complex on the bacterial surface (R-$POCd^+$) played an important role and amounted to 10–20% of the total Cd adsorption. The CA-SCM provided an adequate fit to the adsorption isotherms of Cd on the composite at pH 6 and pH 8, with V_Y values of 4.3 and 2.4, respectively (Fig. S6). Figure 4 depicts the distribution of the total adsorbed Cd between the composite fractions. Montmorillonite played a dominating role in Cd sorption on the composite over the whole pH range studied. The percentage for the adsorption of Cd on

montmorillonite and *B. subtilis* in the composite at pH 6 was 71.4% and 28.6%, respectively. The V_Y value ranging from 0.1 to 20 can generally be considered a good fit. Overall, within the constructs of FITEQL SCM, CA-SCM is adequate to describe the Cd adsorption behavior on the surface of the composite.

3.5. Distribution of Cd on montmorillonite–*B. subtilis* composite by XAS.

Since the model successfully described Cd adsorption on bacteria-clay composite at pH > 5, herein we selected pH 6 samples to investigate whether model predictions match well with the EXAFS prediction. Linear combination fitting (LCF) procedure has been successfully applied to obtain the partitioning of metal adsorption on bacteria-mineral composites (Du et al., 2016; Moon and Peacock, 2012; Templeton et al., 2003). This approach is based on the intermediate adsorption behavior of metals between the end-member component. The Cd K-edge (EXAFS) spectra of montmorillonite, *Bacillus subtilis* and their composite are shown in Fig. 5. A few differences between the spectrum of mineral and bacteria are pronounced at *k*-values of 6-10 Å^{-1}. We were able to produce excellent fits to the Cd-composite spectra with a linear combination of Cd-adsorbed montmorillonite and Cd-adsorbed *B. subtilis* clusters (*R*-factor < 0.1). Linear combination results for the distribution of total adsorbed Cd by the composite yielded a ratio of 69.1%:30.9% for montmorillonite and bacterial cells, respectively. This ratio closely approaches the value obtained from model speculation, which is 71.4%:28.6%.

4. Discussions

A number of investigators have employed CA-SCM to describe metal adsorption onto

mineral–bacteria composites (Alessi and Fein, 2010; Moon and Peacock, 2013; Song et al., 2009). However, to the authors' knowledge, this is the first information on the modelling of Cd adsorption by 2:1 clay mineral–bacteria composites. The species and distribution of Cd on the surface of montmorillonite–*B. subtilis* composite were modeled using CA-SCM in this study. Cadmium was found to be adequately described by adsorption to the nominally assigned RCOOH and POH sites, and the X^- and SOH groups on the surface of montmorillonite–*B. subtilis* composite. Our results imply that all these groups have to be considered for a successful simulation of Cd adsorption on 2:1 clay mineral-bacteria mixtures, compared to ferrihydrite-bacteria composites where, of the bacterial component, only carboxyl (RCOOH) groups were found to be responsible for heavy metal adsorption over the entire pH range studied (Moon and Peacock, 2013). The model of Cd adsorption on montmorillonite–*B*. subtilis composite in our study suggested that X_2Cd was the major species on the composite at pH < 4. Interestingly, montmorillonite played a dominant role in Cd sorption on the composite (the mass ratio of montmorillonite to bacteria was 87.5%:12.5%) over the entire pH range studied. However, the contribution to Cu adsorption from the components of a ferrihydrite–bacteria mixture with a mass ratio of 82%:18% was dependent on pH (Moon and Peacock, 2013). Bacteria and ferrihydrite governed Cu adsorption at low and high pH values, respectively. The montmorillonite has a permanently charged XH site, which provides a certain level of adsorption capacity independent of pH, whereas the ferrihydrite-bacteria composites to which the authors are contrasting their work possess only amphoteric sites (Moon and Peacock, 2013). Our data revealed that the

percentage of total adsorbed Cd on montmorillonite in the composite was in the range of 87.3–69.1% from pH 3 to 8 (Figure S7). These results suggest that the bacteria fraction in the composite plays an increasingly important role in the retention of cadmium ions from pH 3 to 8, although slight decreases in Cd attachment were observed for the bacteria from pH 4 to 5. Some of the Cd ions may have been transferred from the montmorillonite surface to the bacteria in the composite with the rise of pH.

The modelled distribution of Cd on individual components in our montmorillonite–*B. subtilis* composite was supported by the EXAFS investigations at pH 6. The ratio of Cd adsorption onto montmorillonite to that of the bacterial cells present in the composite as obtained from EXAFS spectra analysis closely coincides with the value obtained from model speculation. Both the model simulation and EXAFS observation from our study suggested that the fate of Cd is largely affected by the presence of montmorillonite in soils and sediments, particularly in locations where the mineral exists as the major colloidal component. Our 2:1 clay–bacteria system is different from the 1:1 clay–bacteria system reported by Alessi and Fein (2010), where they found that the majority of Cd is predicted to occur onto the permanent structural site of the kaolinite component only below pH 4 in a kaolinite–*B. subtilis* mixture dominated by the mineral fraction (75%), and *B. subtilis* contribute nearly 58% of the total reactive site. Templeton et al. (2003) reported that 71% and 29% of Pb ions were adsorbed by goethite and bacteria in a goethite–bacteria composite with a mass ratio of 70% : 30% at pH 7. Moon and Peacock (2012) found that the distribution of Cu adsorption between ferrihydrite and bacteria fractions in a ferrihydrite–bacteria

composite (with a mass ratio 65% : 35%) was 80% : 20% at pH 6.4. Our work thus corroborates the findings of Moon and Peacock (2012) who predict that, in mineral-organic composites dominated by the mineral component, the mineral will be responsible for the majority of the heavy metal adsorption and the composites will behave approximately additively. Moreover, this study has extended their work which was based on iron (hydr)oxide-organic composites, to clay mineral-organic composites. The established models from these investigations may provide a universal rule to predict the behavior of trace metals in more complicated ecosystems bearing mineral–organic complexes.

Environmental Implication

Although surface complexation modeling (SCM) has been widely applied to describe trace metal adsorption behaviors on various soil solid components, how to apply it in complex systems is still challenging. The present results indicate that Cd adsorption behaviors on montmorillonite-bacteria composite is successfully described by CA-SCM model, except for some deviations at pH < 5. Current SCM models might be useful for the prediction of the distribution of Cd between solid and solution phases in a variety of settings. Soils and various sediments are composed of clay minerals, organic matter and microorganisms. It is critical to model Cd adsorption and availability at the interface of multi-components interactions which is fundamental for the risk evaluation of Cd-contaminated environments, especially those in temperate regions such as Alfisos and Mollisos which are dominated by 2:1 clays. Secondly, the fact that

the distribution of Cd between the end-member component is dependent on pH, has important implication for Cd mobility. The adsorbed Cd complexes, either outer-sphere or inner-sphere, may exhibit different exchange or desorption behaviors during the changes of environmental factors, e.g., cations, redox potential. The relative mobility of clay– and organic –adsorbed Cd might differ. Under this premise, mineral-organic composite is a suitable analogue for a good predictor of the mobility and thus eventual fate of Cd in natural environments. Lastly, our study has implications for the remediation of Cd contaminant soils and sediments where 2:1 phyllosilicates dominate the mineral composition, in particular, when various organic agents are applied, e.g., straw, manure or engineering microorganisms. These substances are easily bound to soil mineral surface. In these cases, it is vital to consider the fate, mobility of heavy metals with respect to mineral-organic composites, in addition to pure mineral phases.

5. Conclusions

In this study, we developed surface complexation model for Cd(II) adsorption on montmorillonite, *B. subtilis*, and their composite. The Cd adsorption behavior onto the surface of the composite can be described by a component additivity approach (CA-SCM). Underestimation was observed for the model prediction at pH < 5. The X_2Cd, $SOCd^+$, $R-COOCd^+$, and $R-POCd^+$ were the predominant species of Cd adsorbed on the surface of montmorillonite–*B. subtilis* composite. Montmorillonite played a more important role for the binding of Cd ions in the mineral–bacteria composite over the ranges of pH 3 to 8. The distribution of adsorbed Cd between the montmorillonite and

bacteria fractions in the montmorillonite–*B. subtilis* composite as predicted by CA-SCM closely coincided the results obtained from the EXAFS spectra analysis.

Acknowledgements

References

Akafia, M. M., Reich, T. J. and Koretsky, C. M.: Assessing Cd, Co, Cu, Ni, and Pb sorption on montmorillonite using surface complexation models. Appl. Geochem., 26, 154–157, 2011.

Alessi, D. S. and Fein, J. B.: Cadmium adsorption to mixtures of soil components: Testing the component additivity approach. Chem. Geol., 270, 186–195, 2010.

Angove, M. J., Johnson, B. B. and Wells, J. D.: Adsorption of cadmium(II) on kaolinite. Colloid Surface. A, 126, 137–147, 1997.

Benedicto, A., Degueldre, C. and Missana, T.: Gallium sorption on montmorillonite and illite colloids: Experimental study and modelling by ionic exchange and surface complexation. Appl. Geochem., 40, 43–50, 2014.

Borrok, D. M. and Fein, J. B.: The impact of ionic strength on the adsorption of protons, Pb, Cd, and Sr onto the surfaces of Gram negative bacteria: testing non-

electrostatic, diffuse, and triple-layer models. J. Colloid Interface Sci., 286, 110–126, 2005.

Borrok, D., Fein, J. B. and Kulpa, C. F.: Proton and Cd adsorption onto natural bacterial consortia: Testing universal adsorption behavior. Geochim. Cosmochim. Ac., 68, 3231–3238, 2004.

Bradbury, M. H., Baeyens, B., Geckeis, H. and Rabung, T.: Sorption of Eu(III)/Cm(III) on Ca-montmorillonite and Na-illite. Part 2: Surface complexation modelling. Geochim. Cosmochim. Ac., 69, 5403–5412, 2005.

Christl, I., Milne, C. J., Kinniburgh, D. G. and Kretzschmar, R.: Relating ion binding by fulvic and humic acids to chemical composition and molecular size. 2. metal binding. Environ. Sci. Technol., 35, 2512–2517, 2001.

Chu, Z., Liu, W., Tang, H., Qian, T., Li, S., Li, Z. and Wu, G.: Surface acid-base behaviors of Chinese loess. J. Colloid Interface Sci., 252, 426–32, 2002.

Daughney, C. J., Fowle, D. A. and Fortin, D.: The effect of growth phase on proton and metal adsorption by *Bacillus subtilis*. Geochim. Cosmochim. Ac., 65, 1025–1035, 2001.

Dong, W. and Wan, J.: Additive surface complexation modeling of uranium(VI) adsorption onto quartz-sand dominated sediments. Environ. Sci. Technol., 48, 6569–77, 2014.

Du, H., Chen, W., Cai, P., Rong, X., Dai, K., Peacock, C. L. and Huang, Q.: Cd(II) sorption on montmorillonite-humic acid-bacteria composites. Sci. Rep., 6, 19499, 2016.

Du, Q., Sun, Z. X., Forsling, W. and Tang, H. X.: Acid–base properties of aqueous illite surfaces. J. Colloid Interface Sci., 187, 221–231, 1997.

Fein, J. B., Fowle, D. A., Daughney, C. J., Yee, N. and Davis, T. A.: A chemical equilibrium model for metal adsorption onto bacterial surfaces. Geochim. Cosmochim. Ac., 61, 3319–3328, 1997.

Fein, J. B., Boily, J. F. and Yee, N.: Gorman-Lewis, D.; Turner, B. F., Potentiometric titrations of *Bacillus subtilis* cells to low pH and a comparison of modeling approaches. Geochim. Cosmochim. Ac., 69, 1123–1132, 2005.

Fomina, M. and Gadd, G. M.: Biosorption: current perspectives on concept, definition and application. Bioresour. Technol., 160, 3–14, 2014.

Fowle, D. A. and Fein, J. B.: Competitive adsorption of metal cations onto two gram positive bacteria: Testing the chemical equilibrium model. Geochim. Cosmochim. Ac., 63, 3059–3067, 1999.

Gustafsson, J. P., Persson, I., Oromieh, A. G., van Schaik, J. W., Sjostedt, C. and Kleja, D. B.: Chromium(III) complexation to natural organic matter: mechanisms and modeling. Environ. Sci. Technol., 48, 1753–61, 2014.

He, J. and Chen, J. P.: A comprehensive review on biosorption of heavy metals by algal biomass: materials, performances, chemistry, and modeling simulation tools. Bioresour. Technol., 160, 67–78, 2014.

Herbelin, A. L. and Westall, J. C.: FITEQL:a computer program for the determination of chemical equilibrium constants from experimental data. Report. 94-01. Department of Chem, Oregon State University, Corvallis, 1999.

Hohl, H. and Stumm, W.: Interaction of Pb^{2+} with hydrous γ - Al_2O_3. J. Colloid Interface Sci., 55, 281–288, 1976.

Hong, Z., Chen,W., Rong, X., Cai, P., Dai, K. and Huang, Q.: The effect of extracellular polymeric substances on the adhesion of bacteria to clay minerals and goethite. Chem. Geol., 360-361, 118–125, 2013.

Hong, Z., Rong, X., Cai, P., Dai, K., Liang, W., Chen, W. and Huang, Q.: Initial adhesion of *Bacillus subtilis* on soil minerals as related to their surface properties. Eur. J. Soil. Sci., 63, 457–466, 2012.

Ikhsan, J., Wells, J. D., Johnson, B. B. and Angove, M. J.: Surface complexation modeling of the sorption of Zn(II) by montmorillonite. Colloid Surface. A, 252, 33–41, 2005.

Kenney, J. P. and Fein, J. B.: Cell wall reactivity of acidophilic and alkaliphilic bacteria determined by potentiometric titrations and Cd adsorption experiments. Environ. Sci. Technol., 45, 4446–4452, 2011.

Kim, S. S., Min, J. H., Lee, J. K., Baik, M. H., Choi J. W. and Shin, H. S.: Effects of pH and anions on the sorption of selenium ions onto magnetite. J. Environ. Radioact., 104, 1–6, 2012.

Koopal, L. K., Saito, T., Pinheiro, J. P. and van Riemsdijk, W. H.: Ion binding to natural organic matter: General considerations and the NICA–Donnan model. Colloid Surface. A, 265, 40–54, 2005.

Lackovic, K., Angove, M. J., Wells, J. D. and Johnson, B. B.: Modeling the adsorption of Cd(II) onto goethite in the presence of citric acid. J. Colloid Interface Sci., 269,

37–45, 2004a.

Lackovic, K., Wells, J. D., Johnson, B. B. and Angove, M. J.: Modeling the adsorption of Cd(II) onto kaolinite and Muloorina illite in the presence of citric acid. J. Colloid Interface Sci., 270, 86–93, 2004b.

Landry, C. J., Koretsky, C. M., Lund, T. J., Schaller, M. and Das, S.: Surface complexation modeling of Co(II) adsorption on mixtures of hydrous ferric oxide, quartz and kaolinite. Geochim. Cosmochim. Ac., 73, 3723–3737, 2009.

Liu, R. X., Song, Y. H. and Tang, H. X.: Application of the surface complexation model to the biosorption of Cu(II). Adsorpt. Sci. Technol., 31, 1–16, 2013.

Liu, W. X., Sun, Z. X., Forsling, W., Du, Q. and Tang, H. X.: A comparative study of surface acid-base characteristics of natural illites from different origins. J. Colloid Interface Sci., 219, 48–61, 1999.

Milne, C. J., Kinniburgh, D. G., van Riemsdijk, W. H. and Tipping, E.: Generic NICA-Donnan model parameters for metal-ion binding by humic substances. Environ. Sci. Technol., 37, 958–971, 2003.

Moon, E. M. and Peacock, C. L.: Adsorption of Cu(II) to *Bacillus subtilis*: A pH-dependent EXAFS and thermodynamic modelling study. Geochim. Cosmochim. Ac., 75, 6705–6719, 2011.

Moon, E. M. and Peacock, C. L.: Adsorption of Cu(II) to ferrihydrite and ferrihydrite–bacteria composites: Importance of the carboxyl group for Cu mobility in natural environments. Geochim. Cosmochim. Ac., 92, 203–219, 2012.

Moon, E. M. and Peacock, C. L.: Modelling Cu(II) adsorption to ferrihydrite and

ferrihydrite–bacteria composites: Deviation from additive adsorption in the composite sorption system. Geochim. Cosmochim. Ac., 104, 148–164, 2013.

Ravel, B. and Newville, M.: ATHENA, ARTEMIS, HEPHAESTUS: data analysis for X-ray absorption spectroscopy using IFEFFIT. J. Synchrotron Radiat., 12, 537–541, 2005.

Reich, T. J., Das S., Koretsky, C. M., Lund, T. J. and Landry, C. J.: Surface complexation modeling of Pb(II) adsorption on mixtures of hydrous ferric oxide, quartz and kaolinite. Chem. Geol., 275, 262–271, 2010.

Schaller, M. S., Koretsky, C. M., Lund, T. J. and Landry, C. J.: Surface complexation modeling of Cd(II) adsorption on mixtures of hydrous ferric oxide, quartz and kaolinite. J. Colloid Interface Sci., 339, 302–9, 2009.

Soltermann, D., Baeyens, B., Bradbury, M. H. and Fernandes, M. M.: Fe(II) uptake on natural montmorillonites. II. surface complexation modeling. Environ. Sci. Technol., 48, 8698–705, 2014.

Song, Y. T., Swedlund, P., Singha, N. and Swift, S.: Cadmium(II) speciation in complex aquatic systems: A study with ferrihydrite, bacteria, and an organic Ligand. Environ. Sci. Technol., 43, 7430–7436, 2009.

Templeton, A. S., Spormann, A. M. and Brown, G. E.: Speciation of Pb(II) Sorbed by *Burkholderia cepacia*/Goethite Composites. Environ. Sci. Technol., 37, 2166–2172, 2003.

Tertre, E., Castet, S., Berger, G., Loubet, M. and Giffaut, E.: Surface chemistry of kaolinite and Na-montmorillonite in aqueous electrolyte solutions at 25 and 60 °C:

Experimental and modeling study. Geochim. Cosmochim. Ac., 70, 4579–4599, 2006.

Tournassat, C., Neaman, A., Villieras, F., Bosbach, D. and Charlet, L.: Nanomorphology of montmorillonite particles: Estimation of the clay edge sorption site density by low-pressure gas adsorption and AFM observations. Am. Mineral., 88, 1989–1995, 2003.

Wang, Z. and Giammar, D. E.: Mass action expressions for bidentate adsorption in surface complexation modeling: theory and practice. Environ. Sci. Technol., 47, 3982–96, 2013.

Wang, Z., Lee, S. W., Catalano, J. G., Lezama-Pacheco, J. S., Bargar, J. R., Tebo, B. M. and Giammar, D. E.: Adsorption of uranium(VI) to manganese oxides: X-ray absorption spectroscopy and surface complexation modeling. Environ. Sci. Technol., 47, 850–858, 2013.

Weng, L. P., Van Riemsdijk, W. H. and Hiemstra, T.: Cu^{2+} and Ca^{2+} adsorption to goethite in the presence of fulvic acids. Geochim. Cosmochim. Ac., 72, 5857–5870, 2008.

Yee, N. and Fein, J. B.: Cd adsorption onto bacterial surfaces: A universal adsorption edge? Geochim. Cosmochim. Ac., 65, 2037–2042, 2001.
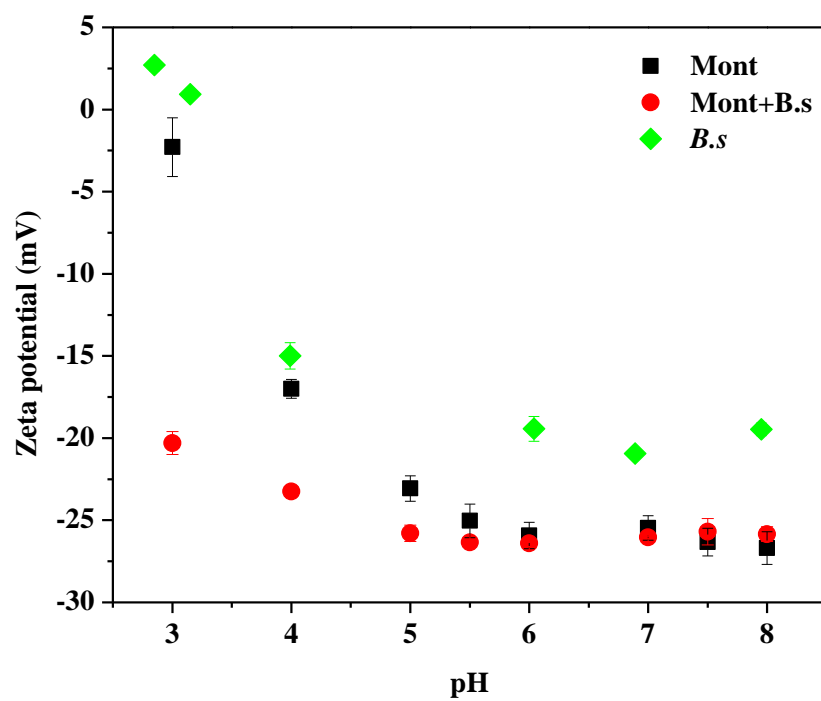
Figure Captions

Figure 1. Zeta potential of montmorillonite, *B. subtilis*, and montmorillonite–*B. subtilis* composite at different pH values.

Figure 2. Adsorption of Cd(II) to montmorillonite, *B. subtilis*, and montmorillonite–*B. subtilis* composite as a function of pH in the presence of 0.01 M $NaNO_3$ (symbols are data points and lines are model fits). The sorbent and initial Cd concentration is 1 g L^{-1} and 10 ppm, respectively.

Figure 3. Speciation diagrams for Cd (II) adsorption onto montmorillonite–*B. subtilis* composite at 28 ℃ in the presence of 0.01 M $NaNO_3$, calculated from the surface complexation models (filled squares represent the experimental adsorption data). Cd(II) :10 ppm, composite: 0.875 g L^{-1} Mont +0.125 g L^{-1} *B. subtilis*.

Figure 4. Distribution of the total adsorbed Cd between montmorillonite and *B. subtilis* fractions in the composite predicted by CA-SCM (symbols are data points, lines are model fits) at 28 ℃ in the presence of 0.01 M $NaNO_3$. Cd(II) :10 ppm, composite : 0.875 g L^{-1} Mont +0.125 g L^{-1} *B. subtilis*.

Figure 5. Normalized Cd K-edge k^3-weighted EXAFS spectra of *B. subtilis* (a), montmorillonite (b) and montmorillonite–*B. subtilis* composite (c) at pH 6.Dotted (blue) line display the best 2-component linear combination fit.

Figure 1. Zeta potential of montmorillonite, *B. subtilis*, and montmorillonite–*B. subtilis* composite at different pH values.
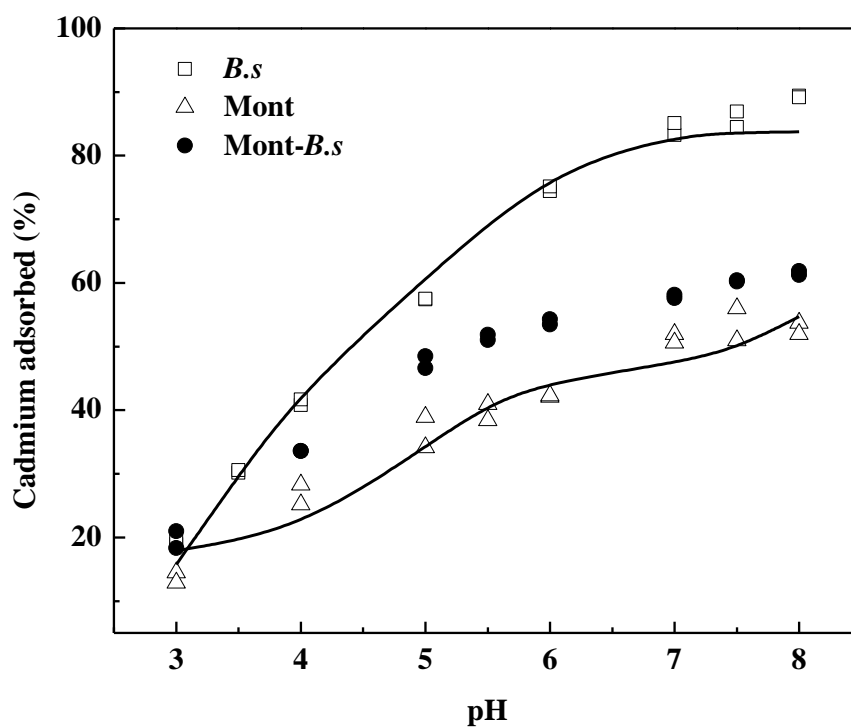
Figure 2. Adsorption of Cd(II) to montmorillonite, *B. subtilis*, and montmorillonite–*B. subtilis* composite as a function of pH in the presence of 0.01 M NaNO$_3$ (symbols are data points and lines are model fits). The sorbent and initial Cd concentration is 1 g L^{-1} and 10 ppm, respectively.
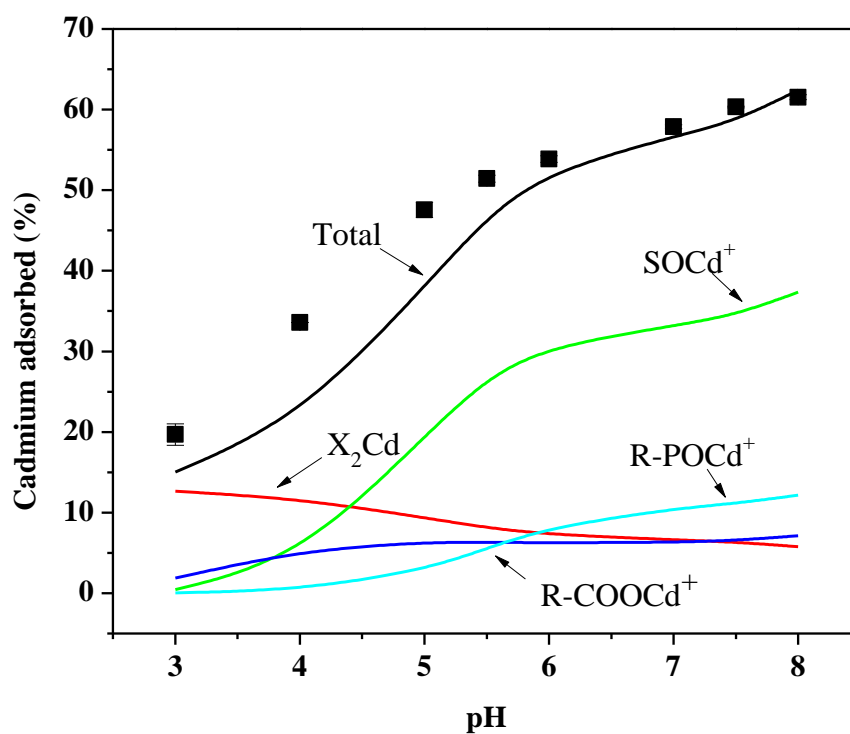
Figure 3. Speciation diagrams for Cd (II) adsorption onto montmorillonite−*B. subtilis* composite at 28 ℃ in the presence of 0.01 M NaNO$_3$, calculated from the surface complexation models (filled squares represent the experimental adsorption data). Cd(II) :10 ppm, composite: 0.875 g L^{-1} Mont +0.125 g L^{-1} *B. subtilis*.
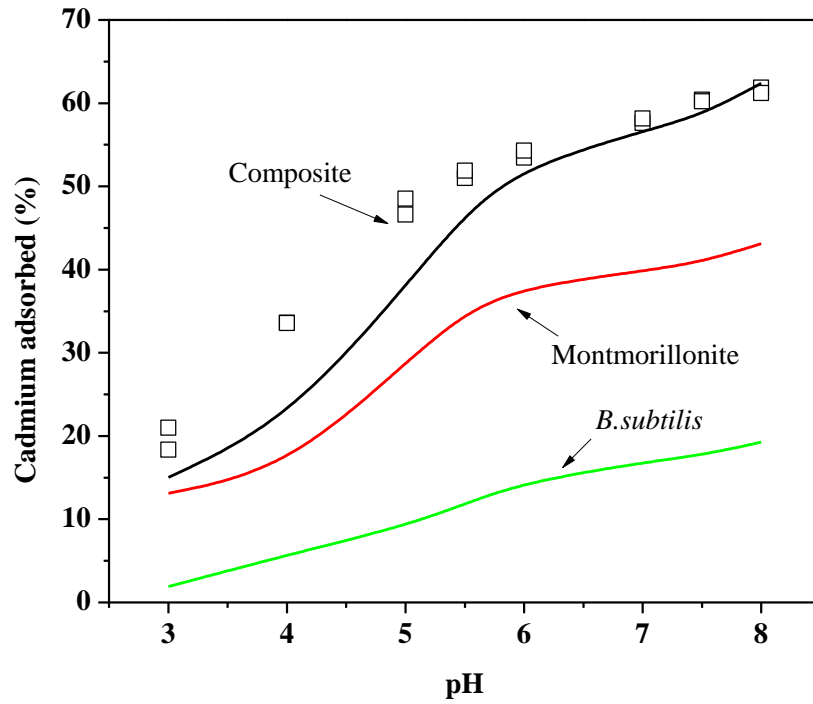
Figure 4. Distribution of the total adsorbed Cd between montmorillonite and *B. subtilis* fractions in the composite predicted by CA-SCM (symbols are data points, lines are model fits) at 28 °C in the presence of 0.01 M $NaNO_3$. Cd(II) :10 ppm, composite : 0.875 g L^{-1} Mont +0.125 g L^{-1} *B. subtilis*.
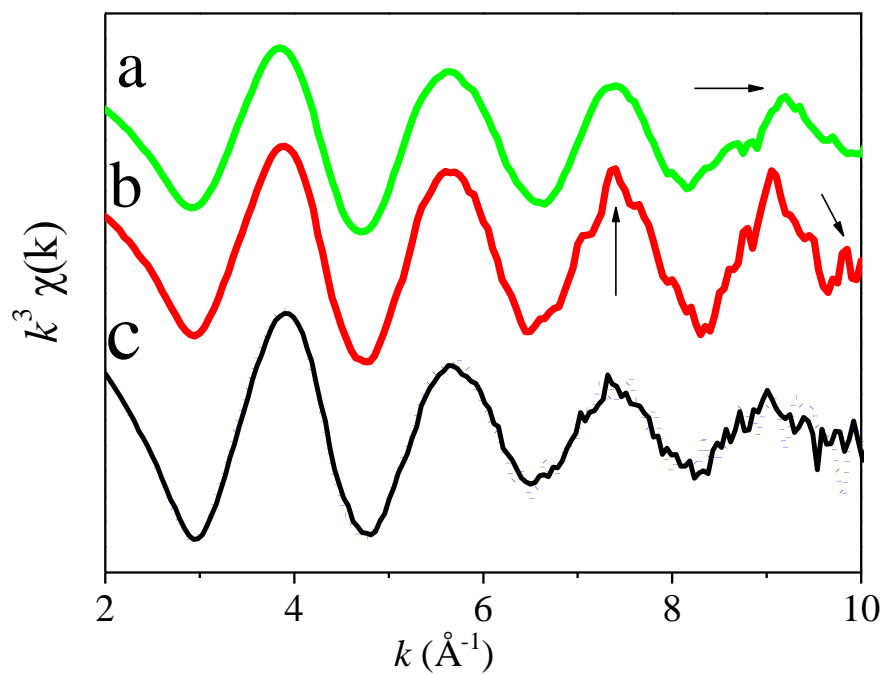
Fig. 5. Normalized Cd K-edge k^3-weighted EXAFS spectra of *B. subtilis* (a), montmorillonite (b) and montmorillonite–*B. subtilis* composite (c) at pH 6. Dotted (blue) line display the best 2-component linear combination fit.

Table 1 Surface complexation model parameters for Cd(II) sorption on montmorillonite–*B. subtilis* composite.

Surface area (m^2/g)		422.6 [b]
Total concentration of sites (mmol/g)		
SOH		0.13 [b]
WOH		0.50 [b]
X$^-$		0.37 [b]
R-COOH		0.09 [b]
R-POH		0.07 [b]
Specific capacitance (F/m^2)		5.54 [b]
Surface reactions		
LogK$_{XH}$	$X^- + H^+ \Leftrightarrow XH$	-2.2 [a]
LogK$_{XNa}$	$X^- + Na^+ \Leftrightarrow XNa$	1.4 [a]
LogK$_{SO^-}$	$SOH \Leftrightarrow SO^- + H^+$	-4.83±0.06 [a]
LogK$_{SOH2^+}$	$SOH + H^+ \Leftrightarrow SOH_2^+$	1.86±0.06 [a]
LogK$_{WO^-}$	$WOH \Leftrightarrow WO^- + H^+$	-8.36±0.08 [a]
LogK$_{R-COO^-}$	$R\text{-}COOH \Leftrightarrow R\text{-}COO^- + H^+$	-3.32±0.08 [a]
LogK$_{R-PO^-}$	$R\text{-}POH \Leftrightarrow R\text{-}PO^- + H^+$	-5.38±0.02 [a]
LogK$_{X2Cd}$	$2X^- + Cd^{2+} \Leftrightarrow X_2Cd$	8.30±0.04 [a]
LogK$_{SOCd^+}$	$SOH + Cd^{2+} \Leftrightarrow SOCd^+ + H^+$	-1.68±0.005 [a]
LogK$_{R-COOCd^+}$	$R\text{-}COO^- + Cd^{2+} \Leftrightarrow R\text{-}COOCd^+$	2.54±0.005 [a]
LogK$_{R-POCd^+}$	$R\text{-}PO^- + Cd^{2+} \Leftrightarrow R\text{-}POCd^+$	2.87±0.02 [a]

[a] Fixed at those determined for montmorillonite-bacteria composite (obtained from Tables S1 and S2)

[b] Calculated using the surface site densities or surface areas or the specific capacitance of the end-member montmorillonite and *B. subtilis* weighted to the mineral:bacteria mass ratio of 7:1.

Supporting Information

Surface complexation modeling of Cd(II) sorption to montmorillonite, bacteria, and their composite

Ning Wang[1,2]*, Huihui Du[1,2]*, Qiaoyun Huang[1,2]**, Peng Cai [1,2], Xingmin Rong[2] and Wenli Chen[1,**]

[1]State Key Laboratory of Agricultural Microbiology, Huazhong Agricultural University, Wuhan 430070, China.

[2] Key Laboratory of Arable Land Conservation (Middle and Lower Reaches of Yangtze River), Ministry of Agriculture, College of Resources and Environment, Huazhong Agricultural University, Wuhan 430070, China.

*These authors contributed equally to this work.

**Corresponding author: Q. Huang, E-mail: qyhuang@mail.hzau.edu.cn; W. Chen, wlchen@mail.hzau.edu.cn; Tel: +86-27-87671033; Fax: +86-27-87280670

Determination of SSA in aqueous.

According to the Tournassat et al. (2003), the specific surface area (SSA) of clay minerals measured by BET is recognized as the basal surface area + edge surface area. However, a particle is supposed to form nearly 20 stacked layers in the dehydrated state during the gas adsorption experiment, whereas it is estimated to be composed of only 1 or 2 layers in aqueous suspension. Herein in our experiments, this "interlayer surface area" must be taken into account. According to the estimation of Tournassat et al. (2003), the basal, interlayer, edge and total surface area of a Na-MX80 clay is 26.6, 753, 8.5 and 788 m^2/g, respectively. The basal + edge surface area for the montmorillonite used in this study is 60.2 m^2/g. If we assume the "interlayer surface area" is 753 m^2/g, the total surface area in aqueous phase should be ~813 m^2/g. Therefore we set the SSA to be 800 m^2/g in this study. In comparison to the values obtained from gas adsorption method, this value may reflect, to a large extent, the realistic situation in aqueous system.
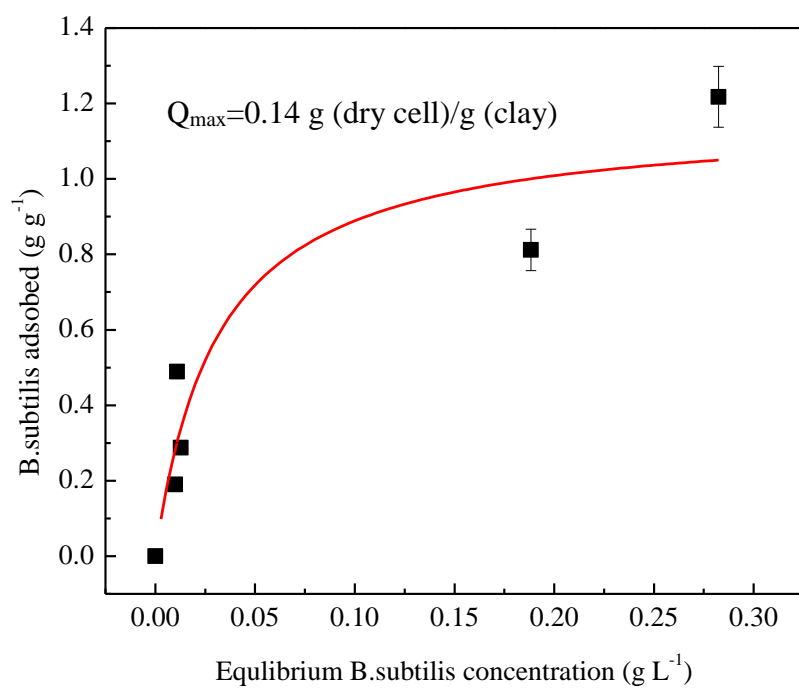
Figure S1. Adsorption of *B. subtilis* (wet) onto montmorillonite at pH 8, 28 ℃,

(An inoic strength of 0.01 M was provided by NaNO₃, the solid line represents fit

curves for Langmuir equations. The ratio of wet to dry weight biomass is 9:1).
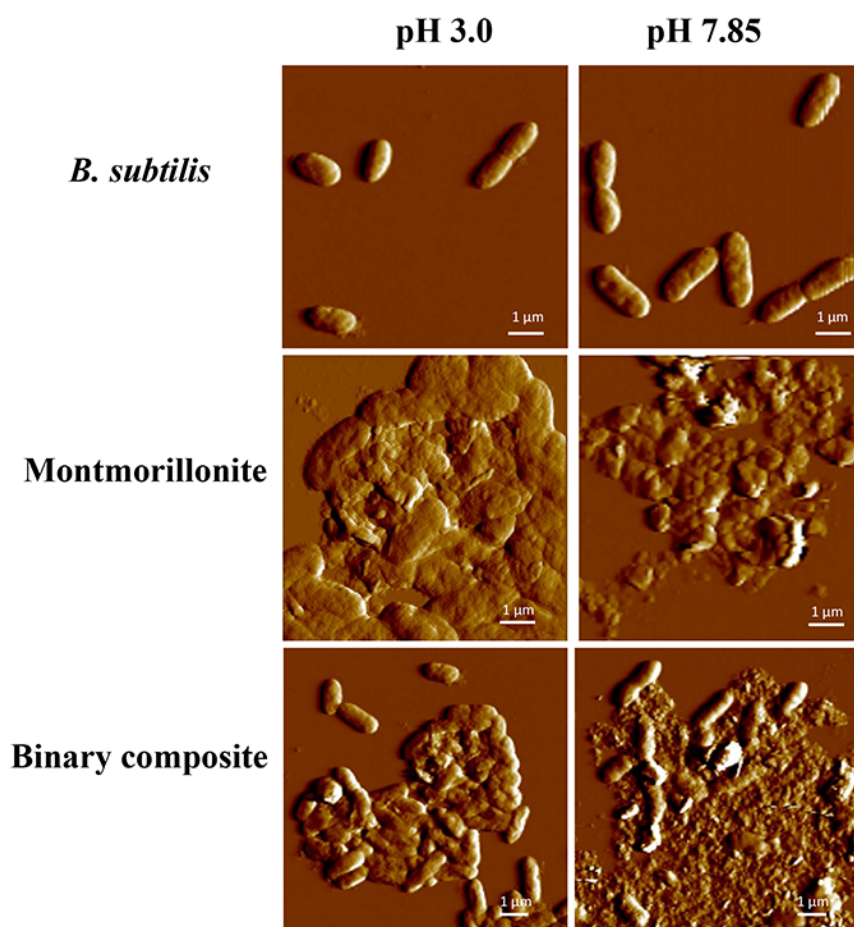
Figure S2. AFM image of *B.subtilis*, montmorillonite and montmorillonite-*B.subtilis* composite at pH 3.0 and pH 7.85. Morphology measurements of the composite was followed the procedure outlined by Huang et al. (2015).
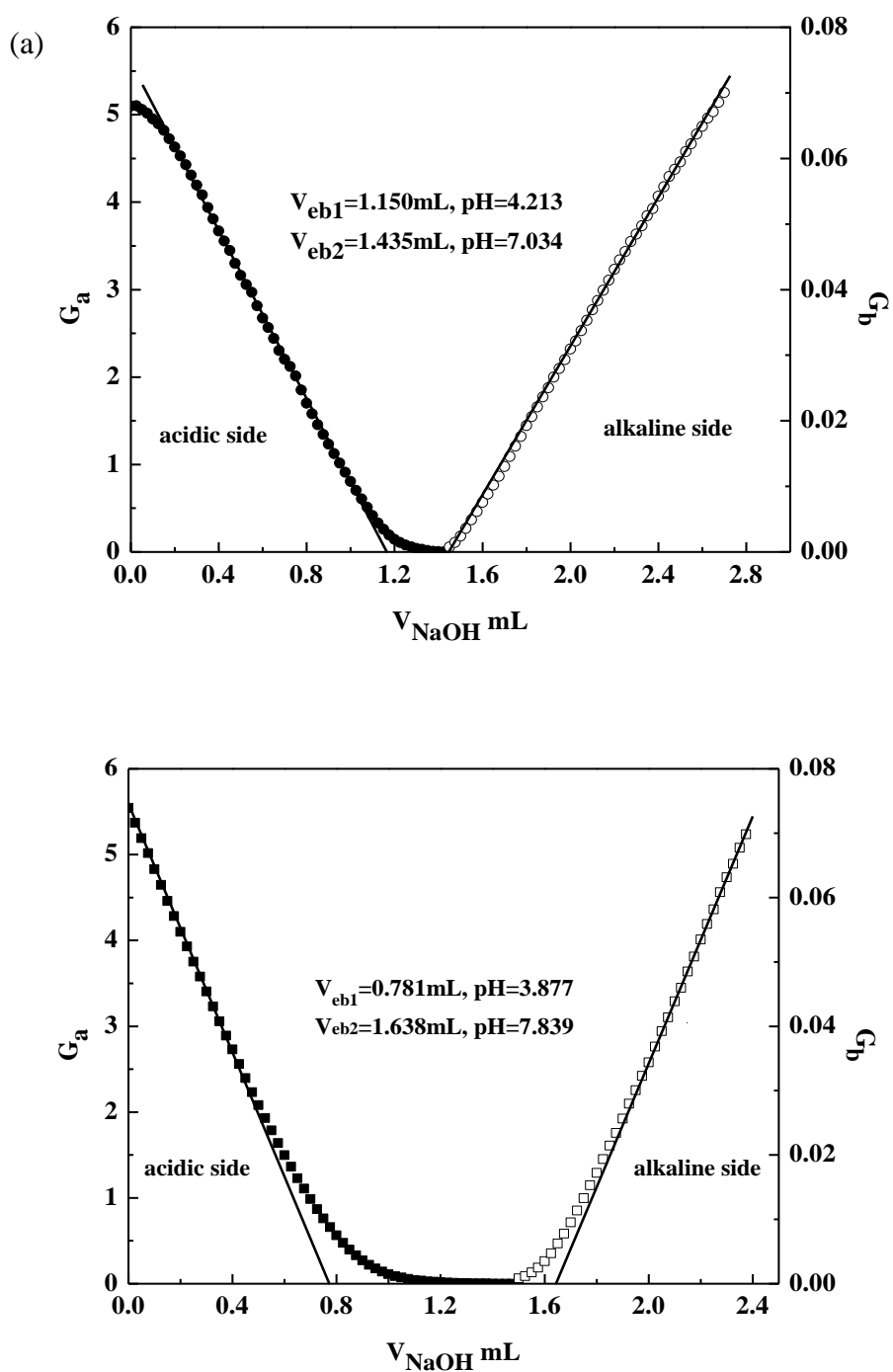
(a)

V_{eb1}=1.150mL, pH=4.213
V_{eb2}=1.435mL, pH=7.034

acidic side

alkaline side

G_a

G_b

V_{NaOH} mL

V_{eb1}=0.781mL, pH=3.877
V_{eb2}=1.638mL, pH=7.839

acidic side

alkaline side

G_a

G_b

V_{NaOH} mL

Figure S3. Gran plots of titration systems with 1 g L^{-1} montmorillonite (a) and *B. subtilis* (b) in 0.01 M $NaNO_3$ solution. The open and filled squares denote the titration data for the sample on the acidic side and on the alkaline side, respectively. The solid line represents the tangential line of the titration curve.
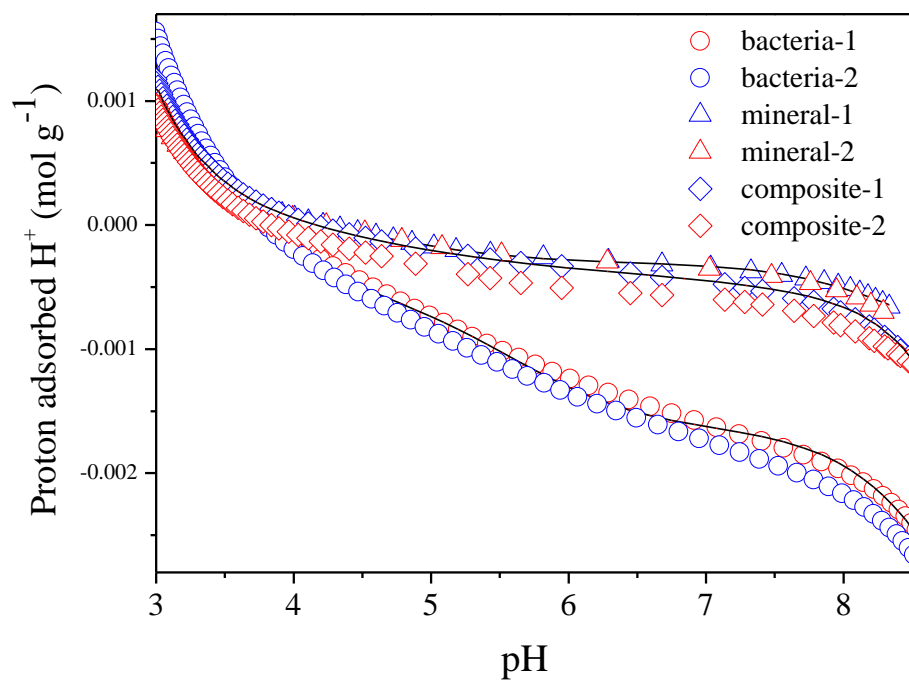
Figure S4. Potentiometric titration data of montmorillonite (a), *B. subtilis* (b) and

montmorillonite-*B. subtilis*(c) in 0.01M NaNO₃ solution at 25 ℃ (symbols are data
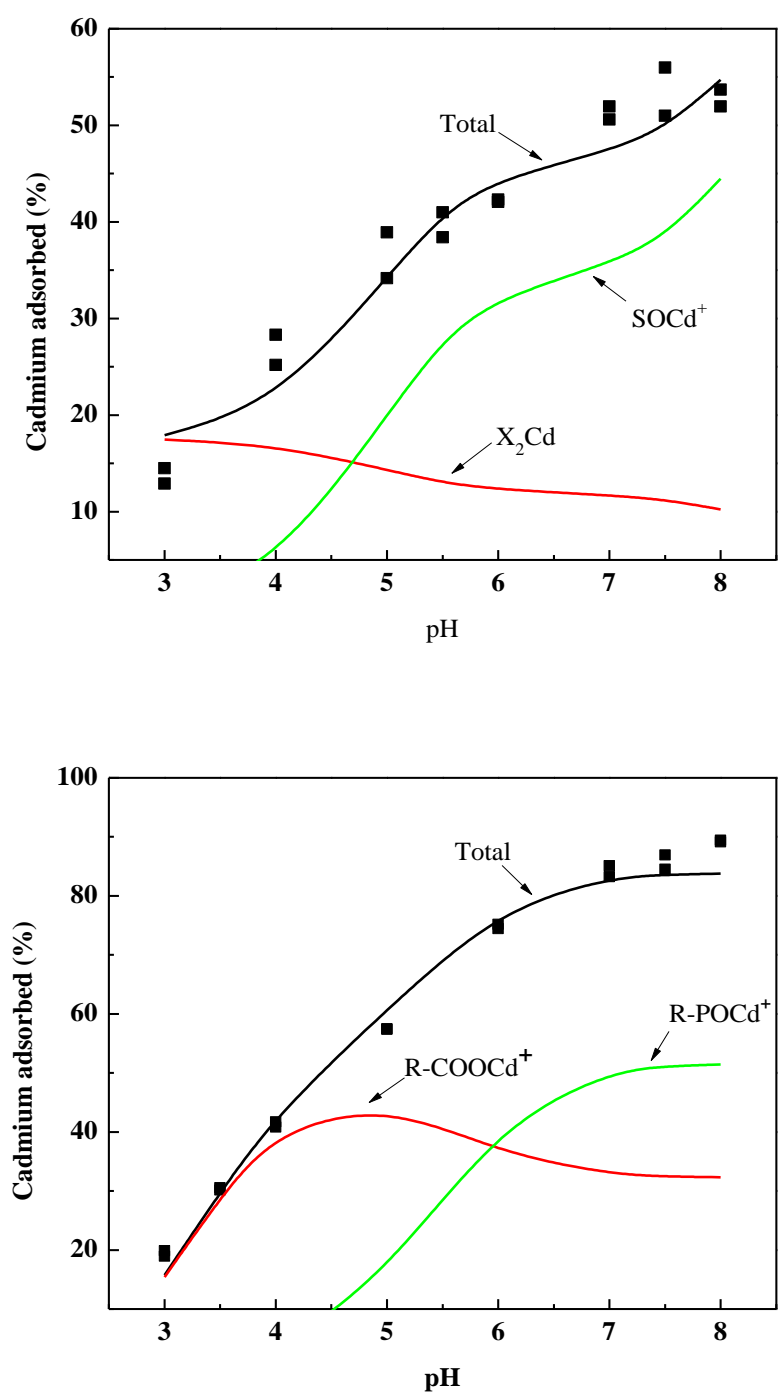
points, line are model fits).

Figure S5. Speciation diagrams for cadmium adsorption onto montmorillonite (a) and

B. subtilis (b) at 28 ℃, calculated from the surface complexation models (filled
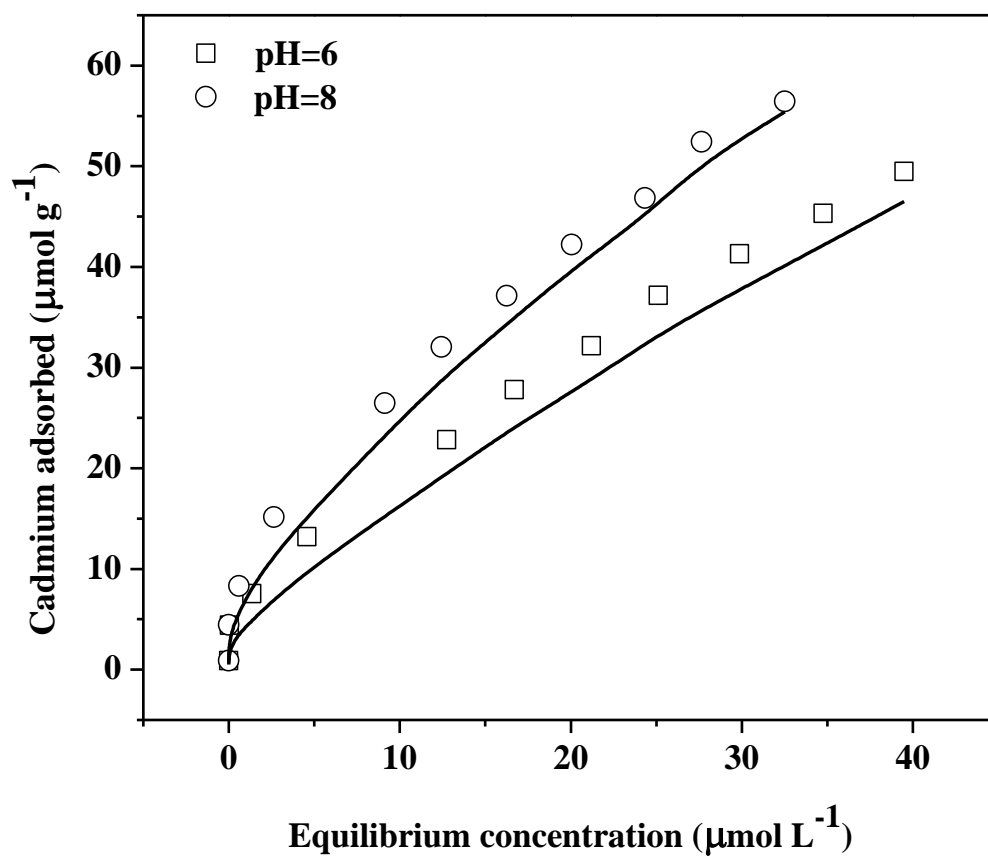
squares represent the experimental adsorption data).

Figure S6. Adsorption isotherms of Cd on montmorillonite–*B. subtilis* composite (1 g L^{-1}) at different pH values in the presence of 0.01 M NaNO$_3$ (symbols are data points and lines are model fits).
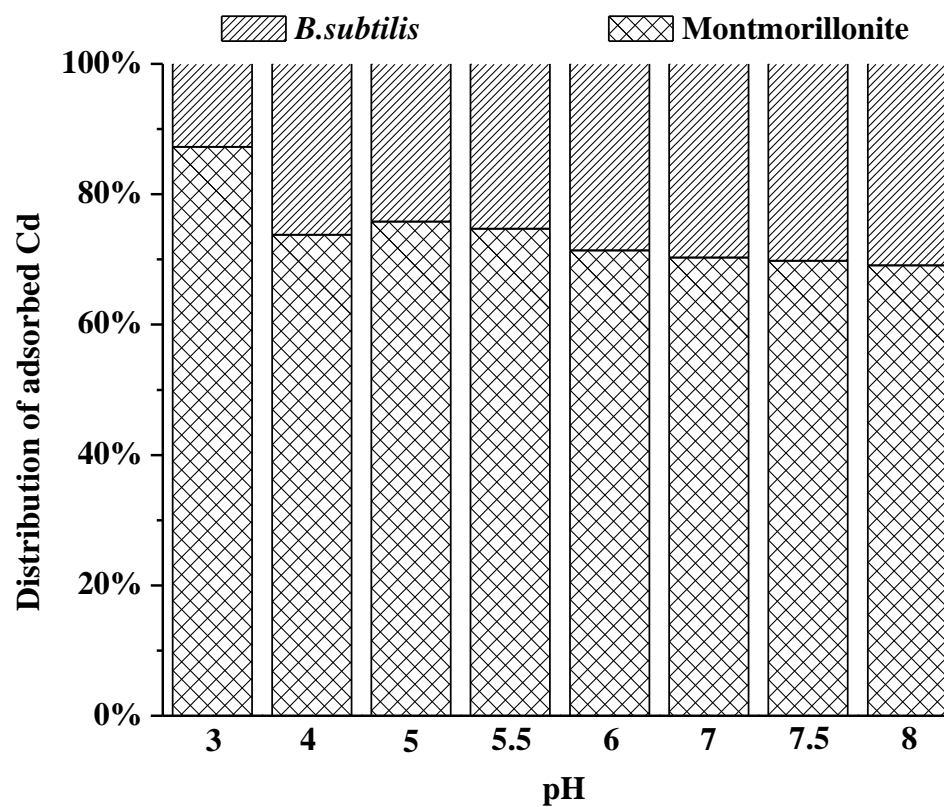
Figure S7. Distribution ratio of total adsorbed Cd between montmorillonite and *B. subtilis* at different pH values in the composite determined from model prediction.

Table S1. Surface complexation model parameters for Cd(II) sorption on

montmorillonite.

Surface area (m^2/g)		800[a]
Total concentration of sites (mmol/g)		
SOH		0.30[b]
WOH		1.16[b]
X^-		0.87[a]
Specific capacitance (F/m^2)		4.5[a]
Surface reactions		
$LogK_{XH}$	$X^- + H^+ \iff XH$	-2.2[a]
$LogK_{XNa}$	$X^- + Na^+ \iff XNa$	1.4[a]
$LogK_{SO^-}$	$SOH \iff SO^- + H^+$	-4.83±0.06[b]
$LogK_{SOH2^+}$	$SOH + H^+ \iff SOH_2^+$	1.86±0.06[b]
$LogK_{WO^-}$	$WOH \iff WO^- + H^+$	-8.36±0.08[b]
$LogK_{X2Cd}$	$2X^- + Cd^{2+} \iff X_2Cd$	8.30±0.04[b]
$LogK_{SOCd^+}$	$SOH + Cd^{2+} \iff SOCd^+ + H^+$	-1.68±0.005[b]

[a] Fixed at those determined for montmorillonite (Tertre et al., 2006 and Soltermann et al., 2014).

[b] Determined from fitting potentiometric titration data.

Table S2. Surface complexation model parameters for Cd(II) sorption on *B. subtilis*.

Surface area (m^2/g)		140
Total concentration of sites (mmol/g)		
R-COOH		0.161 ± 0.03[a]
R-POH		0.123 ± 0.001[a]
R-OH		1.934 ± 0.06[a]
Specific capacitance (F/m^2)		10
Surface reactions		
$LogK_{R\text{-}COO^-}$	$R\text{-}COOH \Leftrightarrow R\text{-}COO^- + H^+$	-3.32 ± 0.08[a]
$LogK_{R\text{-}PO^-}$	$R\text{-}POH \Leftrightarrow R\text{-}PO^- + H^+$	-5.38 ± 0.02[a]
$LogK_{R\text{-}O^-}$	$R\text{-}OH \Leftrightarrow R\text{-}O^- + H^+$	-9.34 ± 0.05[a]
$LogK_{R\text{-}COOCd^+}$	$R\text{-}COO^- + Cd^{2+} \Leftrightarrow R\text{-}COOCd^+$	2.54 ± 0.005[a]
$LogK_{R\text{-}POCd^+}$	$R\text{-}PO^- + Cd^{2+} \Leftrightarrow R\text{-}POCd^+$	2.87 ± 0.02[a]

[a] Determined from fitting potentiometric titration data.

Reference:

Huang, Q., Wu, H., Cai, P., Fein, J. B., and Chen, W.: Atomic force microscopy measurements of bacterial adhesion and biofilm formation onto clay-sized particles. *Sci. Rep.* 5, 16857, 2015.